BACKBONE MODEL FOR MASONRY INFILL WALLS IN STEEL FRAMES BASED ON GOVERNING FAILURE MODE

A. Salehian [(1)], K. Shakeri [(2)], M. Aftabiazar [(3)]

[(1)] *Graduated Student, University of Mohaghegh Ardabil, Ardabil, Iran. salehian_afsaneh@yahoo.com*
[(2)] *Asociante Profesor, University of Mohaghegh Ardabil, Ardabil, Iran.*
[(3)] *Graduated Student, Sharif University of Technology, Tehran, Iran.*

Abstract

The use of infill walls as part of structural system affect strength, stiffness, dynamic response and overall seismic response of the structure. However, inappropriate arrangement of the infill walls may result in twisting when the structure subject to earthquake loading. In the current design standards, an equivalent strut model is prescribed to account for the stiffness and strength of the infills. Backbone model of the equivalent strut is defined based on a bilinear model that includes only effective parameters of infill i.e. ultimate strength and stiffness. Use of this model involves several deficiencies which include inability to track crack propagation, unrealistic behavioral compared to actual response of the infill and in some cases, inappropriate prediction of the infill behavior.

In This study, the main objectives are to identify effective parameters of the frame behavior and to propose a model which accounts for influential parameters. A micro-model of the steel infill frame is first created using the ABAQUS finite element software. The parameters affecting the response of the infill frame were studied after validation of the model against experimental results. A model was then proposed by replacing the infill by an equivalent strut to overcome some of the shortcomings of the current models. The proposed model consists of initial stiffness, cracking point, secondary stiffness, maximum capacity and failure point, which are presented using a multi-linear response. The results showed that the effect of fillers on the behavior of infill frame is so significant. Response of the frame is also influenced by vertical mortar or mortars amongst beams, columns, and infill. Furthermore, the proposed multi-linear model can present a more accurate estimation of the infill behavior.

Keywords: steel frame, masonry infill, micro-modeling, compressive strut, multi-linear model

1. Introduction

Unreinforced masonry infills are widely used in buildings as the exterior walls and partitions. The interaction between infill and frame results in increasing the bearing capacity and stiffness of the composite frame compared to the bare frame. In design, buildings are typically considered as frames consisting of key structural members such as beams, columns, and shear walls; whereas, the role of infill is neglected in the structural analysis and design.

So that consideration of infill role in analysis and design process is necessary. In modern structural design standards, design recommendations and behavioral models have been provided.

The behavioral models proposed by researchers e.g. Mainstone [1] are generally based on the use of an equivalent strut which is represented by the stiffness and ultimate capacity. The proposed models in literature have developed with several simplifications which may results in conservatism in the predication of the overall structural behavior or overestimation of local damages.

In this paper, the effect of influential parameters on interaction between the steel frames and infills are considered. Additionally, recommendations are presented to improve the existing models which includes the initial stiffness, cracking point, and secondary stiffness and failure point.

2. A review of the previous research studies on composite steel frames

Polyakov [2] performed a research on the composite steel and concrete frames under lateral loading. The study concluded that the response of the frame and infill is combined until cracks emerge. Also, the idea of application of diagonal member was proposed in this study. Malcolm Holmes [3] suggested an equivalent strut model based on the experimental studies conducted on steel frames with infills. He proposed the strut width as a coefficient of the infill diameter.

In the study by Stafford Smith [4], the stiffness parameter of the infill-to-frame was used in the modeling and the contact length between the boundary element in the frame and infill wall was determined. In 1968, Stafford Smith conducted an experimental program under uniform distributed load applied on the upper beam of a single-span one-story steel frame. A significant increase in the lateral strength of the infill frame was observed, which depends on the aspect ratio of the infill [5]. In 1977, Bura and Marlic [6] verified the parametric relationship proposed by Smith by means of a testing program performed on the composite steel frames. Mainstone [1] proposed an empirical relationship in order to calculate the width of the equivalent compressive constraint. In this relationship, the concept of equivalent compressive constraint is used. Riddington and Stafford Smith [7] performed finite element analysis on several models of infill frames. Empirical relations have been used to calculate shear, diagonal tensile, and vertical compressive stresses at the center of the wall. They found that the stresses at the center of the infill are strongly influenced by height to the length ratio of the infill. Also, it was found that they are not influenced by the frame stiffness and inter-boundary friction. Stafford Smith and Riddington [8] proposed a method to design the composite steel frames. In this approach, the probability of occurrence of each failure mechanism including shear, tensile and corner failure has been considered. In 1980, Klingner [9] confirmed the final relationship proposed by Mainstone [1].

Liauw and Kwan [10] proposed an empirical relation based on the geometry for the first time. Then, Liauw and Kwan [11] presented a method for plastic analysis based on the laboratory observations and performing nonlinear analyses on the composite frames with regard to the stress redistribution in the infill. In this method, several relationships were proposed to calculate the ultimate load for different failure modes.

Moghaddam and Dowling [12] have conducted some experiments on the composite steel frames which have a distance equal to 10 mm between the boundary elements and infills. Dawe and Seah [13] studied the effects of different factors such as bracing the infill to the column, strength of the mortar, and the friction between the frame and infill. El-Haddad [14] developed a program to analyze the composite frames using the finite element method and fracture mechanics. The program considers several factors including the size and location of the crack, the relative stiffness of the infill and the frame, the geometry of the frame, and the contact length of the infill.

Paulay and Priestley [15] suggested that in analyzing the composite frames, the infill could be considered as the diagonal bracing members with hinge ends. Also, they found that the effective width of the compressive constraint can be considered equal to one quarter of the wall diameter in order to calculate the stiffness of the composite frame. Durrani and Luo [16] found that the strut width can be defined as a factor including the column characteristics in a proportion of the infill diameter. Mosalam et al. [17] conducted a series of quasi-static experiments on the composite steel frames. El-Dakhakhni et al. [18] developed a two-dimensional finite element model to analyze the composite steel frames using the ANSYS finite element program. In this model, the masonry infills with three compressive constraints are replaced by nonlinear element with force-deformation characteristics. This method could easily be used in nonlinear analysis of the solid frames under uniform static lateral loads with peak/maximum bearing capacity. Amato et al. [19] presented a new dimensionless parameter for stiffness ratio and proposed a new relationship for the strut width based on the test results. Skafidaet.al. presented four relationships to obtain the strength of equivalent compressive strut [20]. They used the Decanini and Fantin relationship to compute the strut width [21].

3. Numerical studies

In this study, a numerical simulation has been performed in order to assess the behavior of infill wall. It is felt that there is a need to propose an elaborate model. For the proposed model, the test model by Flanagan and Bennett [22] has been used. Flanagan and Bennett tested a composite single- span one-story steel frame at the University of Tennessee, Knoxville. In this test, the height to span ratio is equal to unity and the loads of the frame are applied based on UBC 1991 specifications. The beam and column sections are W310×52 and W250×45, respectively. The infill dimensions are 2100 × 2100 mm (seven tiles in length and height of infill). The width of brick unit in the hollow form is 20cm (Fig. 1) [22]. Lateral loading, including incremental uniform lateral load is applied to the left corner of the wall using hydraulic jacks. For validation purpose, the frame was modeled using the ABAQUS software and the results were compared with test results. At the loading point, an elastic element is specified. To model the infill, the brick and half-brick are used. Due to the lack of information on the type of mortar, the friction angle and mortar cohesion were obtained based on the engineering judgment .In [22], intervals (0.5 - 0.7) and (30-50) are assumed for the coefficient and friction angle, respectively. A sensitivity analysis was performed which led to a value equal to 0.526 for the cohesion and 42 degree for the friction angle [23]. These values are close to the test results by Flanagan and Bennett .The interaction element called the Drucker - Prager behavioral model, as shown in Table 1, was used to simulate the mortar in the model. The contact element was used between bricks and structural elements. Octagon cube elements were used for modeling the beams and columns. The connection of beam and column was simulated using a tie element. The required restraint was obtained by defining the boundary conditions at column connections. The geometric characteristics of the frame and the material used are given in Fig. 2 and Table 2, respectively. All other parameters can be found in [22].

Table 1 – Characteristics of the brick used in software

Resilient modulus [23]	kg/cm2	56550
Density[23]	kg/cm2	0.00086
Drucker Prager	Angel of Friction	44
	Flow Stress Ratio	1
	Dilation Angle	50

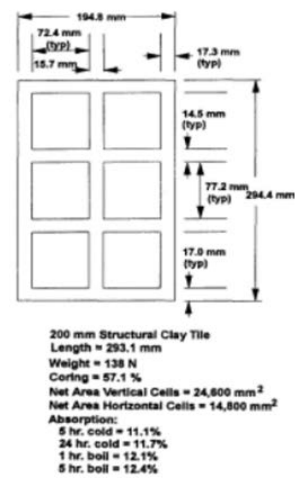

Fig. 1 –Clay tile property [22]

Table 2 – Characteristics of the used material in the laboratory model [23]

Parameter	**Amount**	**Unit**	
f'_{cb}	14.8	MPa	Tile compressive strength
f'_{p}	5.6	MPa	Compressive strength of coherent masonry material
E_x	5390	MPa	Modulus of elasticity of masonry material at x direction
E_y	2160	MPa	Modulus of elasticity of masonry material at y direction
Y	0.14	-	Poisson ratio for masonry material
M	0.5-0.7	-	Mortar friction coefficient
Γ	817	Kg/m^3	Specific weight of masonry material

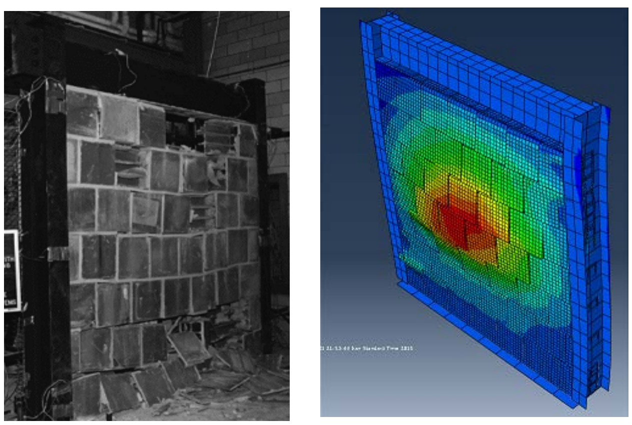

A) B)

Fig. 2 –A) Flanagan and Bennett frame [24], B) finite element model

Fig. 3-A, the chart obtained by interested testing infill under cyclic loading has been shown. Since the testing model is loaded statically and dynamically for studying real behavior of structure under seismic loads, the backbone of hysteresis curve has been used in order to validate pushover analysis. Fig. 3-B shows a comparison between the results obtained from the finite element model of the infill frame and the test results. The comparison reveals a good agreement between the results of finite element and experimental data. The differences seen in the failure stage is due to difference in type of loading.

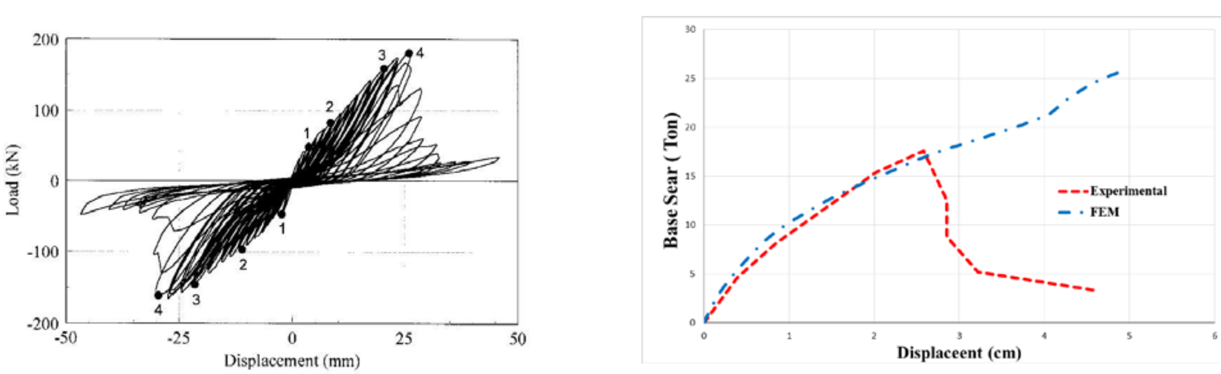

A) B)

Fig. 3 – A) In-Plane Hysteresis Behavior [22] B)The force-displacement curve of the frame [22]

The model verified against the experimental results was used to investigate the response of the composite frame. Characteristics of this model are presented in Table 3:

Table 3 – Characteristics of developed models

Model	Base of Model	Changes made
MainFEM	Flanagan & Bennett model	-
AFM30	Main	Angle of friction 30
AFM40	Main	Angle of friction 40
AFM50	Main	Angle of friction 50
CFM0.5	Main	coefficient of friction mortar 0.5
CFM0.5	Main	coefficient of friction mortar 0.6
CFM0.5	Main	coefficient of friction mortar 0.7
VM	Main	Remove the vertical mortar
CM	Main	Remove mortar between columns and infill
BM	Main	Remove mortar between beam and infill
FEM LH1/2	-	length to the height ratio equal 1/2
FEM LH2	-	length to the height ratio equal 2

4. Sensitivity analysis of the parameters affecting the behavior of the infill

In this section, the sensitivity of the behavior of the infill with respect to the influential parameters are investigated. By this change that dimension of the frame is selected equaled to 3×3 since these dimensions are applicable and close to reality and conventional constructed structures.

4.1 Effect of the friction angle of the mortar

The friction angle is a parameter of the mortar that representing interaction and restraint between mortar and brick. This parameter is presented in the Mohr-Coulomb relation in the form of a tangent, and its value is increased by increasing the mortar strength. In the Chen relation, this parameter depends on the masonry compressive strength. But in this study, only changes in the friction angle on the strength of a masonry unit is investigated without any change in the compressive strength.

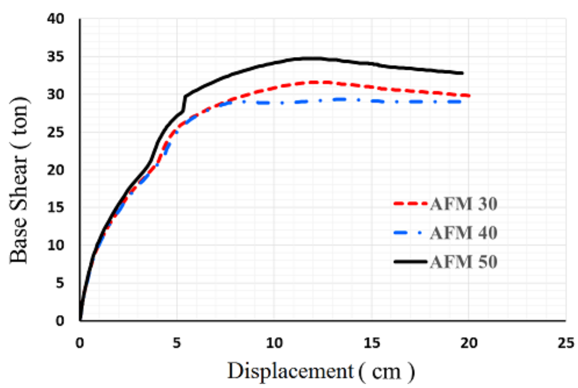

Fig. 4 –investigation of the mortar friction angle

As shown in Fig. 4, as the mortar friction angle increases, the initial stiffness, e.g. primary slope, is not affected but the ultimate capacity and the maximum capacity of the composite infill frame are augmented.

4.2 Effect of the mortar friction coefficient

The friction coefficient is a parameter of the mortar that is presented as a coefficient in the Mohr-Coulomb relationship. In the test specimens used in this study, only variation in the friction coefficient is considered in the strength of the masonry unit. No change was applied to the compressive strength and the friction angle.

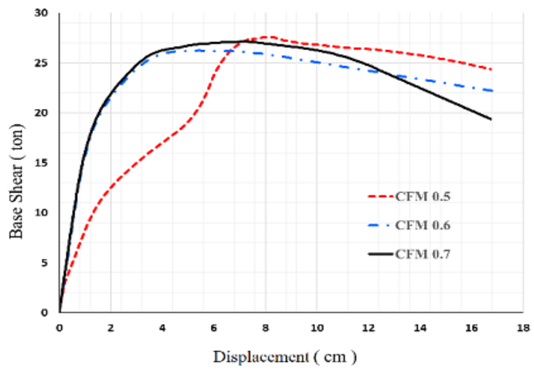

Fig. 5 –investigation of the mortar friction coefficient

As shown in Fig. 5, as the mortar friction coefficient increases, the boundary crack initiates in the plots. Also, the initial stiffness is significantly increased. For the coefficients equal to 0.50 to 0.55, the crack initiates in the diagonal and failure takes place in the corner of the infill. Furthermore, for the friction coefficients between 0.6 and 0.7, these failure modes do not develop. So, the plots show an ultimate failure point. The infill ultimate failure occurs when the coefficient increases for larger lateral loads and smaller displacements. However, the maximum capacity of the composite infill frame has not changed significantly, whereas, the ultimate capacity is reduced as the friction coefficient increases.

4.3 The mortar cohesion

In the masonry infill, different mortars can be used to connect the bricks with two important properties including cohesion and friction coefficient. Cohesion depends on the strength of the masonry unit. Several test results and relationships are available to determine the cohesion value. Based on the Pauly and Priestley [15] relationship, the cohesion strength is obtained from:

$$\tau_0 = 0.04\, f'_m \qquad (1)$$

Where f'_m is the compressive strength of the masonry material.

In this paper, the cohesion of the vertical mortar between bricks and infill, between bricks and columns, and between bricks and beams are investigated.

Based on Fig. 6, it is shown that an increase in cohesion has no significant impact on the initial location of the crack (boundary crack) but it causes to relatively increase the initial stiffness of the infill. However, the maximum capacity of the infill is dramatically increased. Also, it's the impact on the ultimate capacity is lower than the maximum capacity.

Removing the cohesion between mortar and the column does not indicate significant change in the location of the boundary crack. The initial stiffness of the infill is significantly reduced while the crack and ultimate failure of the infill occurred in much lower lateral loads.

By removing the cohesion between mortar and the beam, the infill behavior is independent of cohesion before diagonal crack initiates. Small difference can be seen in the behavior of the infill when the maximum capacity is reached.

In general, if the frame and infill are connected, the cohesion has no significant effect on the behavior of the infill frame. This reason being the separation of the frame and the infill.

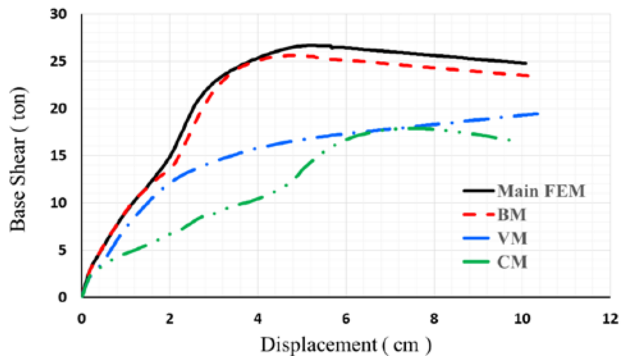

Fig. 6 –investigation of mortar cohesion

4.3 Aspect ratio

To investigate the frame geometry, three samples are considered. The length to the height ratios equal to 1, 0.5 and 2 were called main, LH1/2 and 2LH infills, respectively.

For LH1/2 infill, the displacement corresponding to the infill maximum capacity did not have a significant change, while the maximum capacity and initial stiffness were significantly reduced. The boundary crack occurred in smaller loads and larger displacement. The infill ultimate capacity was less increased with respect to the maximum capacity.

For 2LH infill, the boundary crack occurred in smaller displacement compared to the other infills. No pronounced change was observed for the initial stiffness but the maximum capacity was significantly increased. Diagonal crack, corner failure, and the ultimate failure occurred in larger lateral loads and larger lateral displacements. Noted that the behavior beyond maximum load cannot be interpreted based on the results obtained and need further investigations (Fig 7).

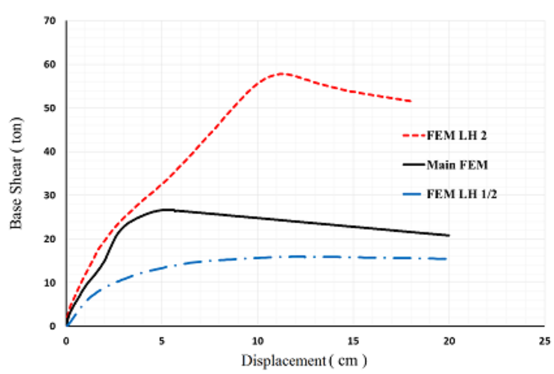

Fig. 7 –Investigation of the height to span ratio of the infill

5. The proposed model

In this section, it has been tried to study all of presented models with regard to acceptable hypotheses based on results of parametric studies in previous sections and to consider the deficient of prior models and finally to choose a comprehensive behavioral model through evaluating previous suggestions. It is obvious that estimation based on the bilinear model has some deficiencies including tracking the locations of the cracks and inappropriate estimation of the response. This model consist of several parameters and key points: initial stiffness, cracking point, secondary stiffness, maximum capacity, and failure point.

As shown in Fig. 8 and Fig. 9, the proposed model was verified. The infill was modeled by two methods including micro-modeling and the equivalent strut. The first method was used for research purpose and the second one was used for engineering applications. The proposed model was based on use of solid element for frame and strut as an equivalent for infill. Characteristics such as area, elastic modulus, and strength of strut are required for definition of this element. To present a comprehensive behavioral model, the results of the equivalent strut and those of the parametric study were plotted and compared. Then, three models from the previous parametric studies were chosen. In order to generalize the proposed relationships, three different span to length ratios were selected.

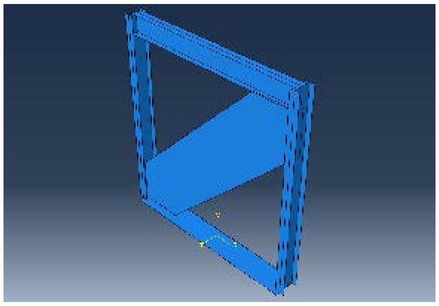

Fig. 8 –modeling of the composite frame

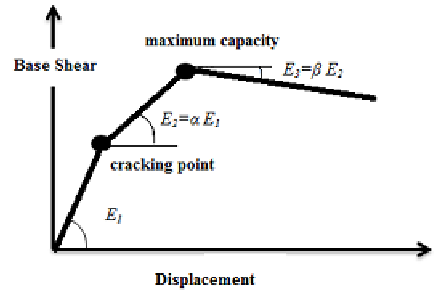

Fig. 9 –Proposed model the equivalent strut

5.1. Initial stiffness

In the models presented so far, the initial stiffness of the infill frame was neglected before separation develops between the frame and infill for simplification. Meanwhile, this assumption is far from reality to obtain the stiffness, period, base shear, and the overall seismic behavior of the structure in the lower levels of loading. For smaller loads, until the crack occurs, the infill act together with the frame and this is confirmed by the stiffness previously obtained. Additionally, due to strut performance of the infill, it is concluded that the use a strut with larger values is appropriate. So that, a coefficient of infill diameter is proposed as the strut width to calculate the initial stiffness and the strength of the masonry unit. Also, the modulus of elasticity of the strut is taken equal to that of the masonry unit. Since the above-mentioned method assumes 0.36 x infill diameter as the strut width, as shown in Fig.10, this method is investigated for the height to span ratio of the strong frame.

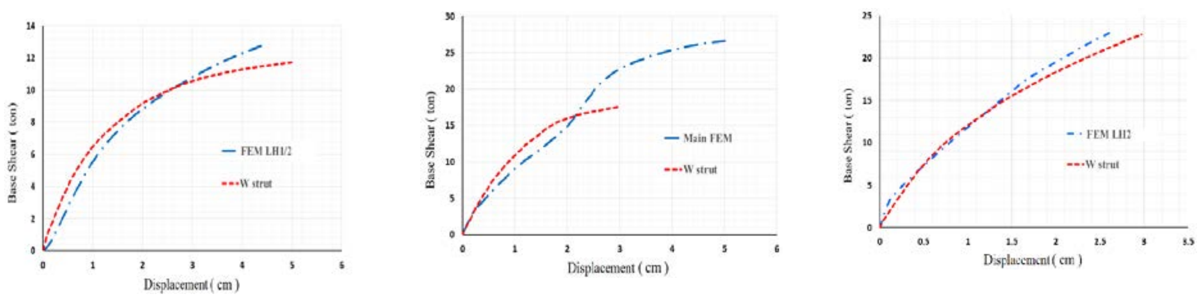

Fig. 10 –Comparing the initial stiffness with the proposed method in different height to span ratios (strong frame)

5.2. Cracking point:

Moghaddam suggested that separation of the frame from the infill developing at the beginning of the first step of failure leading to nonlinear behavior of the composite frame [12]. Few researchers have reported this parameter. This is mainly due to the lack of data. The Mohr-Coulomb relationship is the most important and reliable relationship in order to determine the cracking force. Equation (2) depends on the frame geometric characteristics as well as sliding- mechanical characteristic such as the friction angle, cohesion of the mortar, and masonry unit. =But this is independent of the infill compressive strength. It should be noted that due to the dominant mode and the materials used in practice, it is assumed that the cracking is of the shear type and the tensile mode is neglected (Fig. 11). In this relationships, l and t are length and thickness of infill; H and F_t are exerted force on infill and allowable tensile stress of masonry material, respectively. τ_0 and μ are shear cohesion and frictional coefficient in shear surface, respectively.

$$H_{dc} = \frac{\tau_0 lt}{1.43 - \mu(\frac{0.8h}{l} - 0.2)} \quad (2)$$

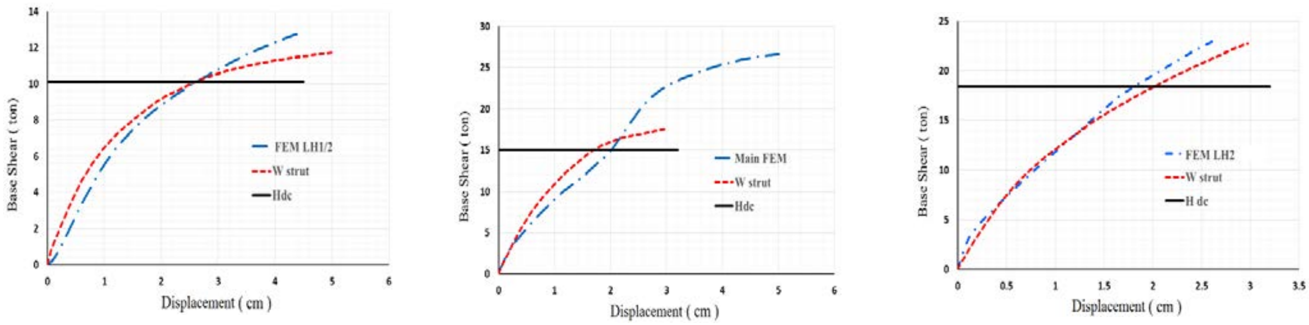

Fig. 11 –Achieving the cracking point in different height to span ratios

5.3. Secondary slope

In multi-linear model, it is not permitted to use a slope parallel to the bilinear models, which are previously presented by others, to obtain the secondary slope. Since all the relationships presented for the strut width are only used to achieve the ultimate capacity , it is possible to use the width strut proposed by Liauw and Kwan since the stiffness obtained from FEMA relations is smaller than the stiffness of the cracking point up to the ultimate capacity. The coefficient α can be obtained using the values of cracking stress $f_{cr})$ and the stress corresponding to the maximum capacity (f_{ymax}) as follow:

$$E_1 = E_m \quad (3)$$

$$E_2 = \frac{E_1 W_d}{W_m} \quad (4)$$

$$A_1 = dt \quad (5)$$

$$A_2 = W_m t \quad (6)$$

$$\alpha = \frac{(f_{ymax} A_2 - f_{cr} A_1)}{(E_1 A_1)(\frac{f_{ymax} A_2}{E_2 A_2} - \frac{f_{cr} A_1}{E_1 A_1})} \quad (7)$$

where, W_d is the strut effective width obtained from the Kalory and Papia [19] relationship and W_m is the effective width proposed by FEMA.

5.4. Ultimate strength

In FEMA 306 [25], it is suggested to use of the strut strength considering the alternative compressive strut. This approach is so common tool while FEMA 356 [26] suggests that the sliding of the infill mortar is the determining factor in ultimate strength of the composite infill frame. Some researchers such as Mohammadi [24] have used the minimum values obtained from the Liauw and Kwan relationship and the shear force in the mortar for the weak frames, whereas, FEMA 306 [25] approach was used for appropriate frames (Fig. 12).

In the proposed model, the strut with a width presented by Mainstone and utilized by FEMA was used in order to achieve the ultimate capacity. The elastic modulus of the infill was defined for the strut. In this study, the strength of the strut was obtained from the following equation and the *S* values obtained from Table 4.

$$f = smf'_m \tag{8}$$

The m value, which is obtained from the combination of the relations presented by Liauw and Kwan [11] and Wood [27], is the smallest value among the following relations:

$$m = \sqrt{\frac{2(M_{pj}+M_{pc})}{\lambda f_m t h^2}} \quad \textbf{(9)} \qquad m = \frac{1}{tan(\theta)}\sqrt{\frac{2(M_{pj}+M_{pb})}{\lambda f_m t h^2}} \quad \textbf{(10)} \qquad m = \frac{4M_{pj}}{f_m t h^2} + \frac{1}{6\max(1,\ tan^2(\theta))} \quad \textbf{(11)}$$

Where, M_{PJ}, M_{PC} and M_{Pb} are plastic moments of beam to column connection, column and beam, respectively. The λ value is equal to:

$$\lambda = 2.66m^3 - 1.37m + 0.406 \leq 0.45 \tag{12}$$

And the m value is equal to:

$$m = \frac{8M_{PJ}}{f'_m lt} \tag{13}$$

Table 4 – the S values

Infill type			**Frame type**
weak	**Intermediate**	**Good**	
0.73	0.73	1	Strong

The coefficients of the Table 4 represent the importance of the strength ratio of the frame to infill such that the S value is approximately taken equal to 1.0 for both the frame and infill are weak or strong. If one of them is weaker than the other one, this ratio is taken equal to 0.7. Note that the parametric study is performed for the hollow brick; so that the relationships are true for the hollow brick masonry materials. Their applications for the solid bricks need more investigations.

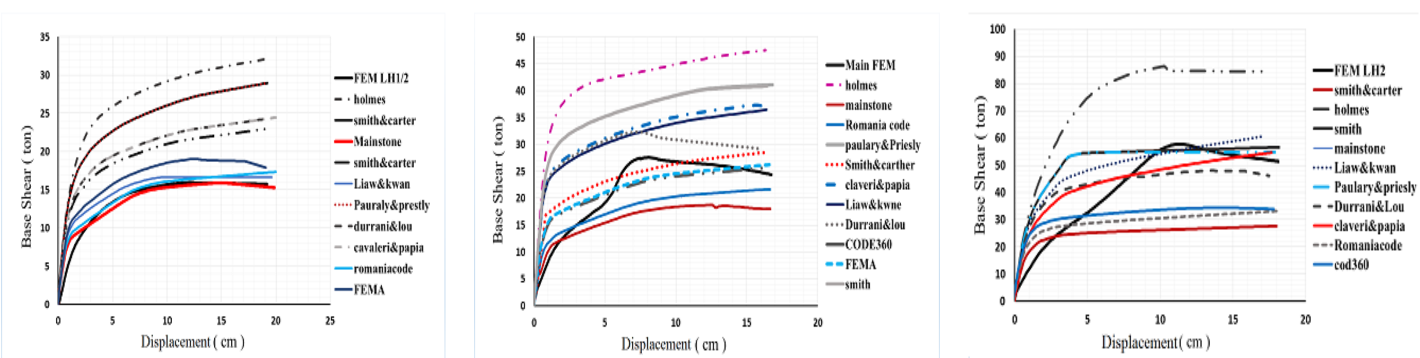

Fig. 12 –Comparing the models proposed for the ultimate capacity with different height to span ratios.

5.5. Ultimate slope (the slope beyond ultimate capacity)

In the previous behavioral models, a boundary was typically selected in order to avoid numerical error. Researchers such as Mehrabi proposes 0.8 times the ultimate capacity as the failure point as is the case in FEMA. In the model prescribed in FEMA, the relative deformation of the composite frame with masonry infill has been proposed equal to 1.5 percent of ultimate point. In the proposed model, FEMA procedure is recommended if the failure point is required.

The proposed multilinear model is compared to the results of finite element model of the composite frame (Fig. 13).

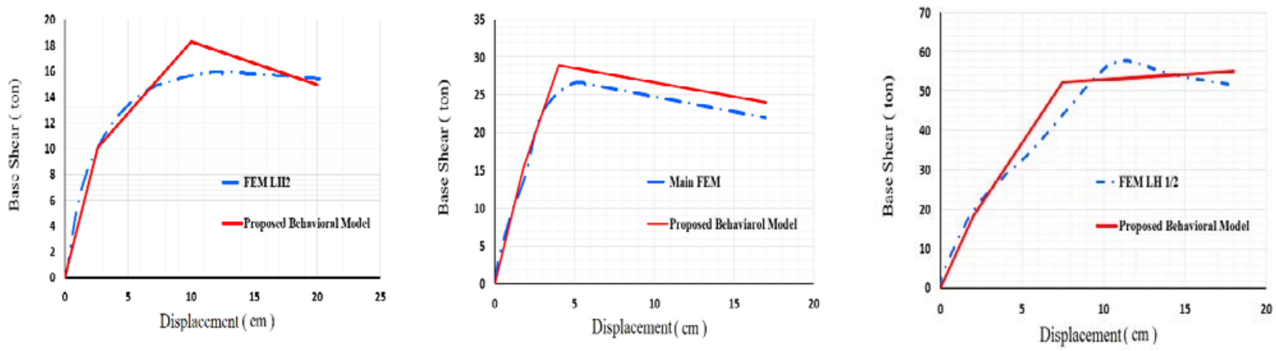

Fig. 13 –Comparing proposed model for infill in steel frames with model obtained by finite element software

6. Conclusion

This study was conducted to investigate the behavior of the unreinforced brick infill in steel frames under the in-plane demands as well as to provide a behavioral model for infill frame based on the dominant failure mode. Parametric studies were performed on micro-models in the ABAQUS software. Considering the parametric studies and previous studies, a model was proposed by replacing the infill by compressive strut. This model includes several parameters and key points including initial stiffness, cracking point, secondary stiffness, and the maximum capacity. This model is capable of realistically estimating of the ultimate capacity. The main findings of this study are summarized as follows:

1) In steel composite frames with masonry fillers, the vertical mortar had a significant impact on the infill frame behavior so that maximum capacity and ultimate bearing capacity increased 37% and 21%, respectively.

3) In composite frames with infill connected to the external columns, the maximum capacity increased up to 33%. But the connection to the upper beam did not have significant effect on the results.

4) The cohesive effect of the mortar used between the infill and columns on the ultimate capacity was negligible and cohesion of the mortar used between infill and the beam on the ultimate capacity was relatively important.

5) As the stiffness is increased, the friction coefficient increases; while, no significant change was observed in maximum capacity but the ultimate capacity is decreased.

6) The maximum capacity increased by increasing the friction angle, while, there was no significant impact was observed on the initial stiffness.

Using strut compressive strength for individual failure mode according to the least calculated strength led to unrealistic values. The combination of the modes during the failure could also be considered in future studies. The relationships prescribed in FEMA356 for the compressive strut strength of the infill predicts the ultimate capacity lesser than the actual values. This relationships, may introduce conservatism due to their lower capacity estimation compared to the actual values but, since its estimated force is small for controlling the infill effect, therefore, they act in the contra-confidence direction.

5. References

[1] Mainstone, R. J., 1971. On the Stiffness and Strengths of Infilled Frames. Proceedings of the Institution of Civil Engineers, Supplement IV, pp 57-90.

[2] Polyakov S.V., 1963. Masonry in Framed Buildings. Translated by G.L. Cairns in. National Lending Library for Science and Technology, Boston Spa, Yorkshire. U.K,

[3] Holmes, M., 1961. Steel Frames with Brickwork and Concrete Infilling. ICE Proceedings (Vol. 19, pp. 473), Telford.

[4] Stafford-Smith B., 1966. Behavior of Square Infilled Frames. J. Struct. Di., ASCE, Vol. 92, No. ST1, pp. 381-403

[5] Stafford-Smith B, 1968. Model Test Result of Vertical and Horizontal Loading of Infilled Frame. J. ACI, 65(8), 618-624.

[6] Bura, HK, .Marlic, S.K., 1977. Behavior of Mortar Infilled Steel Frame under Lateral Load. Building and Environment.

[7] Riddington, J. R.., Stafford Smith, B., 1977. Analysis of Infilled Frames Subjected to Racking with Design Recommendations. The Structural Engineer, Vol.55, No. 6.

[8] Stafford Smith, B., Riddington, J. R., 1978. The design of masonry infilled steel frames for bracing structures. The Structural Engineer, No. 1, Vol. 56B, pp.1-7.

[9] Klingner, R. E. 1980. Mathematical Modeling of Infill Frame. Reinforced Concrete Structure Subjected to Wind and Earthquake Force. ACI SP-63, 1-25.

[10] Liauw T. C., Kwan K. H., 1984. Nonlinear Behavior of Non-Integral Infilled Frames. J Computer and Structure, 18(3).

[11] Liauw T. C., Kwan K. H., 1985. Unified Plastic Analysis for Infilled Frames. J of Struct. Eng., 111(7), 1427-1448.

[12] Moghaddam H. A. Dowling P. J., 1987. The State of The Art in Infilled Frames. ESEE Res. Rep. No 87-2, Imperial Coll. of Sci. and Technol., Civ. Eng. Dept., London, England.

[13] Dawe J. L, Seah C.K, 1989. Out-of-plane Resistance of Concrete Masonry Infilled Panels. Civ. Eng. 16,854-864.

[14] El-Haddad M. H., 1991. Finite Element Analysis of Infilled Frames Considering Cracking and Separation phenomena. Comp Struct, 41(3), 439-447.

[15] Paulay, T. Priestley, M. J. N., 1992. Seismic design of reinforced concrete and masonry buildings. John Wiley and Sons, Inc., New York, NY, USA

[16] Durrani, A. J., Luo, Y. H., 1994. Seismic Retrofit of Flat-Slab Buildings with Masonry Infills. Proc., NCEER Workshop on Seismic Response of Masonry Infills, National Center for Earthquake Engineering Research. Buffalo, NY.

[17] Mosalam K. M., White R. N., Gergely P., 1997. Static response of infilled frames using quasi-static experimentation. J. of Struct. Eng., 123(11), 1462-1469.

[18] El-Dakhakhni W. W. 2003, Three-Strut Model for Concrete Masonry-Infilled Steel Frames. J. of Struct. Eng.

[19] G. Amato, M. Fossetti, L. Cavaleri, M. Papia. 2009. An Updated Model of Equivalent Diagonal Strut for Infill Panels, Euro code 8, Perspectives from the Italian Standpoint Workshop, ,119-128.

[20] Skafida, S., Koutas, L., Bousias, S. N 2014. Analytical Modeling of Masonry Infilled RC Frames and Verification with Experimental Data. Journal of Structures

[21] L.D, Decanini, G.E. Fantin, 1986. Simplified models of Masonry Included in porches. Features lateral stiffness and strength limit state, Argentine Conference on Structural Engineering, Buenos Aires, Argentina, Vol.2, pp.817-836.

[22] Flanagan, R.D.; Bennett, R.M. 1999; Bidirectional Behavior of Structural Clay Tile Infilled Frames, *Journal of Structural Engineering*, Vol, 125, No. 3: Las Vegas.

[23] Bennett, R.M. Boyd, K.A.; Flanagan, R.D. 1997; Compressive Properties of Structural Clay Tile Prisms, *Journal of Structural Engineering*, Vol, 123, No. 7: Las Vegas.

[24] Mohammadi. M. Instructions for seismic evolution and rehabilitation of existing school buildings with infill panels .1393. State organization of school renovation, development and mobilization; research and technical office

[25] Federal emergency management agency, FEMA-306, “evaluation of earthquake damaged concrete and masonry wall buildings”, FEMA, Washington (USA), 1998.

[26] Federal emergency management agency, FEMA-356, “Prestandard and Commentary for the Seismic Rehabilitation of Buildings”, FEMA, Washington (USA), 2000.

[27] Wood, R. H., 1978. Plasticity, Composite Action and Collapse Design of Unreinforced Shear Wall Panels in Frames. In ICE Proceedings (Vol. 65, No. 2, pp. 381-411). Thomas Telford.